Neural Computing and Applications (2023) 35:12583–12598
https://doi.org/10.1007/s00521-023-08395-2

ORIGINAL ARTICLE

YoDenBi-NET: YOLO + DenseNet + Bi-LSTM-based hybrid deep learning model for brain tumor classification

Abdulkadir Karacı[1] · Kemal Akyol[2]

Received: 18 October 2022 / Accepted: 13 February 2023 / Published online: 4 March 2023

Abstract
Brain tumor, which is the deadliest disease in adults, grows rapidly and disrupts the functioning of organs. Brain tumors can be of different types, depending on their shape, texture, and location. The correct detection of these types helps the field specialist to make the correct diagnosis and thus save the patient's life. In this study, a three-stage hybrid new classification framework based on YOLO + DenseNet + Bi-LSTM is proposed to classify glioma, meningioma, and pituitary brain tumor types. In this framework, the brain region is detected first through the YOLO detection algorithm. In the second stage, deep features are extracted from this region via a pre-trained deep learning architecture, and in the final stage, brain tumor classification is performed by way of the Bi-LSTM network which is another deep learning model. The proposed model offers high test accuracies of 99.77% and 99.67%, respectively, for three brain tumor types using hold-out and tenfold cross-validation techniques on a dataset containing 3064 MRI images. With its high performance in validation and test sets, the proposed hybrid model is better than other previous studies and so it can be used as a useful decision support system for field specialists.

Keywords Brain tumor classification · YOLO · DenseNet201 · Bi-LSTM

1 Introduction

Cancer is the most common life-threatening disease today, and among the many types of cancer, the most aggressive form is brain cancer or tumor [1, 2]. The brain is the most complex organ that plays a remarkable role in our daily activities [2, 3]. The brain, the most developed organ of the human body, regulates movement, speech, thoughts, and memories. Type of foreign substance, inflammation, lesion, or any of these in the brain tissue can cause vision and hearing loss, speech impediment, weakness, paralysis, and even death [4]. Uncontrolled growth of tissues in the brain is known as a brain tumor, which is a very serious disease [2]. World Health Organization [5] reported that around 9.6 million people worldwide died from cancer in the year, 2018.

Due to the dire condition of cancer, its abnormal growth, and the complexity of brain structure, timely diagnosis is necessary [6]. Brain tumor, which is one of the increasing causes of death among children and adults, is called cancerous tissues in the brain or a collection of abnormal cells produced by a metastatic process. It reduces the patient's life quality and significantly limits his/her daily activities. Brain tumors are divided into two main categories, benign and malignant. While malignant tumors are cancerous, benign tumors are not [7].

Early diagnosis of a brain tumor and classification according to its specific grades are crucial to effectively treat the tumor [8]. Glioma, the most common type of tumor with the highest mortality rate [9], consists of brain glial cells that support and surround the brain neuron. Almost 33% of all tumors are diagnosed as gliomas. Meningioma occurs in the exterior regions of the brain or in the spinal cord adjacent to the tissues of the meninges [4]. Meningioma is a non-cancerous tumor that grows from the membranes surrounding the brain and spinal cord.

✉ Kemal Akyol
kakyol@kastamonu.edu.tr

[1] Faculty of Engineering, Software Engineering, Samsun University, Samsun, Turkey

[2] Faculty of Engineering and Architecture, Computer Engineering, Kastamonu University, Kastamonu, Turkey

Pituitary tumors develop in the pituitary gland and fall under the category of benign tumors [10].

Accurate tumor diagnosis is a crucial step in disease prognosis and treatment planning. A biopsy is highly invasive, time-consuming, and prone to sampling error [11, 12]. In addition, heterogeneity within the tumor, as well as differences in subjective examinations by field experts, is the main challenges in the histopathological-based tumor grading system (Biopsy) [12, 13].

Timely diagnosis of brain tumors is very important for patient health and treatment planning. Evaluation of brain tumor images is often a time-consuming task for radiologists [14]. Moreover, human decisions are not always correct in this time-consuming process [2]. Magnetic resonance imaging (MRI) scanning is the most used method in neurology to visualize detailed features of the brain and other cranial structures. MRI is useful in visualizing anatomy in three different planes which are axial, coronal, and sagittal [15]. This method is radiation-free and produces images with high resolution and contrast. Therefore, it is the most appropriate imaging method for the noninvasive diagnosis of brain tumor types [16].

The anatomical structure of the brain is complex, and so many problems are encountered such as underfitting, biased results, and overfitting. Hence, developing an expert system to classify brain tumors is a difficult task [17, 18]. It is very important to extract meaningful features from brain tumor images and to perform trial-and-error studies based on machine learning in a successful expert system design. Classification studies in the literature on the detection of whether or not brain MRI images contain tumors can be divided into three categories [7]:

1. Studies in which handcrafted features from tumor sites are fed as input to a traditional classifier or ensemble classifiers.
2. Deep learning-based studies where both feature extraction and classification are performed by a network.
3. Studies with traditional classifiers on deep features extracted from pre-trained deep learning models.

In this study, a three-stage hybrid new classification framework is proposed with the motivation to successfully classify glioma, meningioma, and pituitary brain tumors. The novelty of this study is that it proposes a framework based on YOLO, DenseNet and Bi-LSTM referred as YoDenBi-NET in the paper throughout for the detection of brain tumors. In this study, the region of interest is determined ***with*** YOLO before the original images are sent to the CNN unlike the deep learning studies in the literature. In the second stage, deep features are extracted from the brain region detected by YOLO. In the final stage, these features are sent to the Bi-LSTM network and brain tumor classification is performed.

The contributions of this paper can be summarized as follows:

1. A new deep learning model called YoDenBi-NET, which has not been used in previous studies, is proposed to classify brain tumors.
2. YoDenBi-NET is a three-stage model that uses YOLO to focus on the region of interest, CNN to extract features from this region, and Bi-LSTM to classify with high-success capability.
3. YoDenBi-NET offers a significant classification performance improvement when compared to pre-trained models. Moreover, it is more successful than studies in the literature.

This paper is organized as follows: Sect. 2 presents related works. Section 3 gives detailed information about the material and method. Section 4 includes the results and discussion. Finally, Sect. 5 presents the conclusions and gives information about future works planned.

2 Related work

Brain tumor classification has been extensively studied in the literature with many different models and approaches, so far. It is seen that in some of the feature extraction studies, which is the basic element of classification, handcrafted feature extraction techniques are applied, and in some, deep learning architectures, which are quite outstanding with their successful performances, are used today. Moreover, deep learning studies include the use of built from scratch and pre-trained CNN models and the use of traditional classifiers on deep features extracted from fully connected layers before the last layer of the CNN.

Rehman et al. used AlexNet, GoogLeNet, and VGGNet pre-trained networks to classify brain tumors such as glioma, meningioma, and pituitary and classified the features they extracted through support vector machines and log-based softmax layer. In their study, the authors achieved the highest accuracy of 98.69% using the fine-tuned VGG16 network [19]. In another study, Noreen et al. achieved 99.34% and 99.51% test accuracy, respectively, with the Inception-v3 and DensNet201 networks on the dataset containing three tumor classes [20]. Huang et al. used a complex network-based convolutional neural network to classify brain tumors from magnetic resonance images. The authors reported that the CNN they optimized with random generated graph algorithms and modified activation function had a classification accuracy of 95.49% [21]. Cheng et al. analyzed the efficiency of density histogram, gray level co-occurrence matrix, and a bag of words (BoW) feature extraction methods for brain tumor classification problem. The authors trained the support

vector machines, K nearest neighbor, and K-means algorithms on the features they obtained, and they achieved the highest value of accuracy with 91.14% using the SVM classifier on the BoW features [22]. Gumaei et al. used a regularized extreme learning machine (RELM) for brain tumor classification. After using L2 normalization to extract features to be used in training this classifier, they combined the PCA method with the GIST descriptor. The authors achieved a 94.233% value of accuracy in their studies [23]. Sachdeva et al. classified T1-weighted MR images including astrocytoma, glioblastoma multiform, childhood tumor-medulloblastoma, meningioma, secondary tumor-metastatic, and normal regions brain tumor types. The authors applied the PCA technique to the density and texture features they extracted from the images and achieved 91% accuracy with artificial neural networks [24]. Yin et al. proposed a study that includes background removal, feature extraction, and multilayer perceptual neural network-based classification steps for brain tumor classification. In their proposed study, they improved the classification model with a whale optimization algorithm that includes chaos theory and logistic mapping technique, and they achieved 87% accuracy [25]. Pashaei et al. achieved 93.68% accuracy with the kernel ELM classifier on the features they extracted from the convolutional layers of the CNN for brain MR images [26]. Arı and Hanbay reported that they classified benign and malignant tumors with a 97.18% value of accuracy using the extreme-learning machine-local receptive fields classifier they trained on cranial magnetic resonance images [27]. Özyurt et al. achieved a 98.33% accuracy ratio with the ELM classifier on the features they extracted with AlexNet and SqueezeNet to classify malignant and benign brain tumor types [28]. Byale et al. determined the area of interest using the Gaussian Mixture Model technique on the images, which they removed noises with the adaptive median filter technique, extracted the features with GLCM, and, in the final stage, they achieved 93.33% accuracy with the neural network [29]. Hsieh et al. achieved classification accuracies of 76%, 83%, and 88%, using global, local, and combined features obtained from MRI images that include high and low levels of glioma, respectively [30].

Zia et al. proposed a generalized classification model based on cropping the rectangular window image for brain tumors. The model proposed by the authors includes three stages such as feature extraction based on discrete wavelet transform, features reduction with PCA and classification with SVM [31]. Anaraki et al. optimized the parameters of the CNN they used to classify brain tumors with a genetic algorithm. In addition, they applied a bagging algorithm for reducing the prediction error of the CNN network and obtained 94.2% classification accuracy [32]. Choudhury et al. classified tumor and non-tumor MRI images using CNN with 96.08% accuracy and 2.98% error [33].

In addition, there are studies carried out on the dataset we used in our study, as well. For example, Ismael and Abdel-Qader trained the backpropagation neural network classifier on the features they obtained using a combination of 2D Discrete Wavelet Transform (DWT) and 2D Gabor filter techniques to classify brain tumors in MRI images. The authors achieved 95.66% accuracy on the three-class dataset containing meningioma, glioma, and pituitary brain tumors with their proposed model [34]. Abiwinanda et al. achieved 84.19% accuracy in the classification they performed with the fully connected layer on the features they extracted from the convolution layers of CNN to distinguish glioma, meningioma, and pituitary brain tumors [35]. Sultan et al. tested the CNN-based model they proposed on two different datasets to classify different brain tumors. While the first one includes three classes: meningioma, glioma, and pituitary tumor, the second one includes three grades of glioma (Grade II, Grade III, and Grade IV). The authors achieved 96.13% and 98.7% accuracies, respectively, on these datasets with the deep learning model they proposed [36]. Kumar et al. first performed feature reduction with gray wolf optimization on brain tumor images and obtained 95.23% classification accuracy with multiclass support vector machine on the dataset they obtained [37]. Paul et al. examined the classification performances of convolutional neural networks, fully connected neural networks and random forest algorithms. They used a CNN with two convolution layers each with 64 filters of size 5×5, MaxPool layers, two fully connected layers with 800 neurons, and a Softmax with three neurons in the output layer and achieved 90.26% accuracy [38]. Das et al. classified the brain tumor (glioma, meningioma, pituitary) images which were preprocessed using the Gaussian filter and histogram equalization technique, with a convolutional neural network and achieved a 94.39% test accuracy [39]. Badža and Barjaktarović classified brain tumors with a 22-layers CNN model. The authors tested the generalization ability of their proposed model with subject-wise cross-validation and record-wise cross-validation and achieved a 96.56% accuracy utilizing the tenfold cross-validation and dataset augmented [40].

Mondal and Shrivastava proposed a new activation function called Parametric Flatten-p Mish to improve the performance of their CNN model for brain tumor classification. The authors stated that the activation function they used was able to overcome important disadvantages such as neuron death and bias shifting effect [41]. Shanthi et al. first used image enhancement and noise removal techniques in their proposed hybrid deep neural network model for brain tumor classification. Then, they used adaptive driver optimization to optimize the parameters of the

LSTM for classifying the features extracted from these images [42]. Aamir et al. used the partial least squares method on the features extracted from these images obtained by magnetic resonance imaging with two different deep learning models to detect brain tumors. Following that, they classified the tumor regions they obtained through agglomerative clustering [43] Aurna et al. selected the best two on the basis of accuracy from the five pre-trained models they studied and a proposed CNN model and combined them for feature extraction. They performed the classification of brain tumors by optimizing their proposed two-stage ensemble model [44]. Oksüz et al. presented a region of interest expansion and feature fusion-based study for brain tumor classification. They did this by fusing deep features extracted from tumor regions that included surrounding tissues with pre-trained AlexNet, ResNet-18, GoogLeNet, and ShuffleNet, and shallow features extracted with a shallow network. They then trained the DVM and k-NN classifiers on these features [7]. Vankdothu et al. detected brain tumors in MRI images by using the feature extraction capability of CNNs followed by the classification capability of LSTM. In terms of accuracy, the authors reported that their proposed model outperformed previous CNN and RNN models [45].

3 Material and method

In this study, two hybrid models, Model-1 and Model-2, are proposed to classify meningioma, glioma, and pituitary tumors from brain tumor MRI images. Model-1 is based on YOLO and pre-trained CNN and includes three stages. In the first stage, pre-processing and normalization are applied to the brain images. In the second stage, the brain region is detected and cropped with the YOLO detection algorithm, which is trained to detect the brain region. In the third stage, DenseNet201, ResNet50V2, InceptionV3, VGG16, and VGG19 CNN models are trained on these images and brain tumors are classified with these models. The prominent point in Model-2 is that the Bi-LSTM network is fed with features obtained from the pre-trained CNN models. The most important approach in this model is to increase the classification performance by focusing on the brain region with YOLO. The second important approach is to increase the classification performance through the Bi-LSTM network fed with the features obtained from the previous layer of the fully connected layer of the pre-trained CNN models. Figure 1 presents these models.

The rest of this section presents information about YOLO, pre-trained CNN, and Bi-LSTM for classifying brain tumor types. The dataset used to validate the performance of the models and the details of the performance metrics are given in this section.

3.1 Dataset

In this study, the publicly available T1-weighted CE-Magnetic Resonance Imaging (MRI) dataset [46] was used to evaluate the performance of the proposed models. This dataset was obtained from Nanfang Hospital and General Hospital in China between 2005 and 2010 and it contains 3064 MRI images at 512 × 512 resolution of 233 patients. The dataset includes 3 types of tumors: meningioma (708 images), glioma (1426 images), and pituitary tumor (930 images). These images were taken in three different planes such as sagittal (1025 images), axial (994 images), and coronal plane (1045 images) [22, 40]. It must be noted that satisfactory performance in deep learning depends on the available data. The number of samples in the dataset used in this study is at a satisfactory level, and there is no need to generate synthetic data. Figure 2 shows examples of different tumor types.

3.2 You only look once (YOLO)

Redmon et al. handled object detection as a regression problem differently from other studies and introduced the YOLO model. This model is based on a spatially separated bounding box and associated class probability. mAP (mean average precision) value of this model is two times the mAP of other real-time detectors. YOLO, which is capable of processing video streams in real-time, processes 155 frames per second. YOLO uses features extracted from the entire image to predict each bounding box and simultaneously predicts all bounding boxes in all classes for an image [47].

Each bounding box consists of 5 predictions: x, y, w, h, and confidence. These predictions are encoded as an $S \times S \times (B * 5 + C)$ tensor. Here, width (w) and height (h) are estimated based on the entire image. Each grid cell C estimates the conditional class probabilities, Pr(Classi|Object). The (x, y) coordinates represent the center of the box relative to the boundaries of the grid cell. Each grid cell estimates the confidence score using each B bounding box and $\Pr(\text{Object}) * \text{IOU}_{\text{pred}}^{\text{truth}}$. These confidence scores reveal how confident the model is whether there is an object in the box and also how accurate its prediction is. The confidence estimate represents the Intersection over Union (IoU) between the predicted box and ground truth box. IoU, one of the important metrics used to demonstrate model success in object detection, is the overlap ratio between the target bounding box and the predicted bounding box and is calculated as in Eq. 1 [48].

$$\text{IoU} = \frac{\text{Overlap Area between ground} - \text{truth bounding box and predicted}}{\text{Combined Area between ground} - \text{truth bounding box and predicted}} \quad (1)$$

Another metric used to evaluate the performance of models in object detection is the mean average precision (mAP) given in Eq. 2. In this equation, AP_k is the average precision for class k, and n is the number of classes. The mAP metric compares the detected box with the ground-

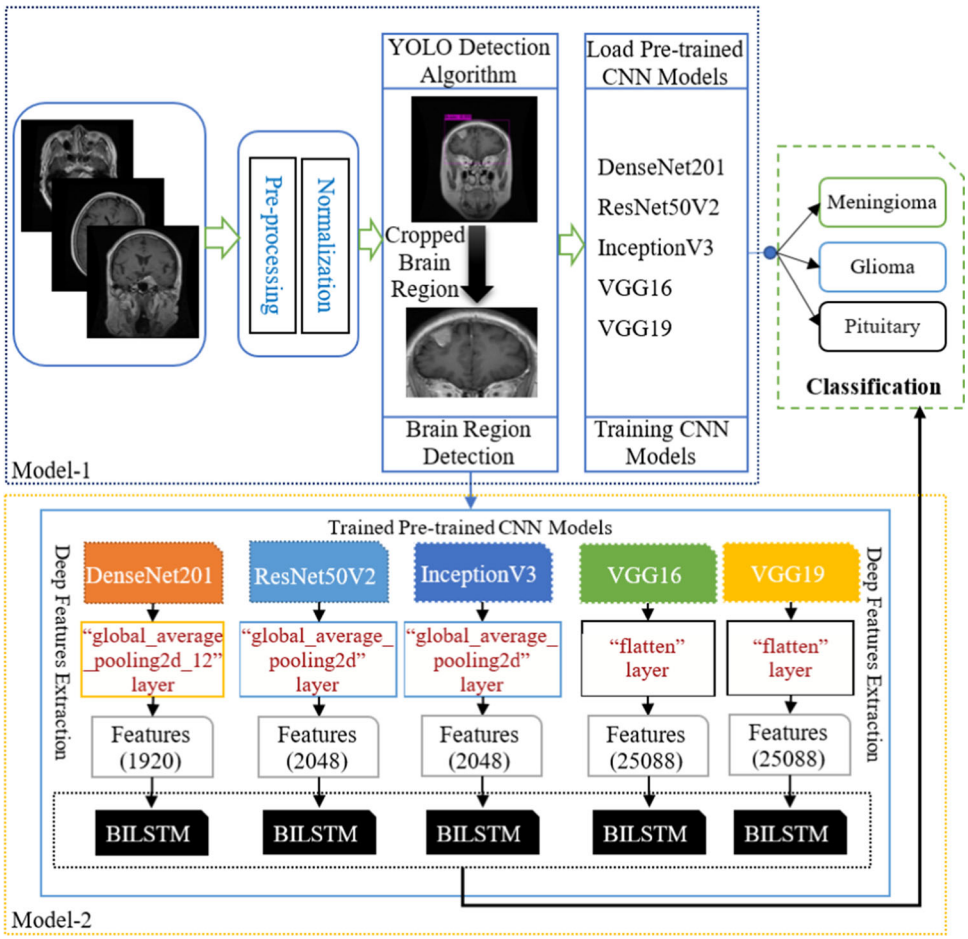

Fig. 1 Overview of the proposed framework

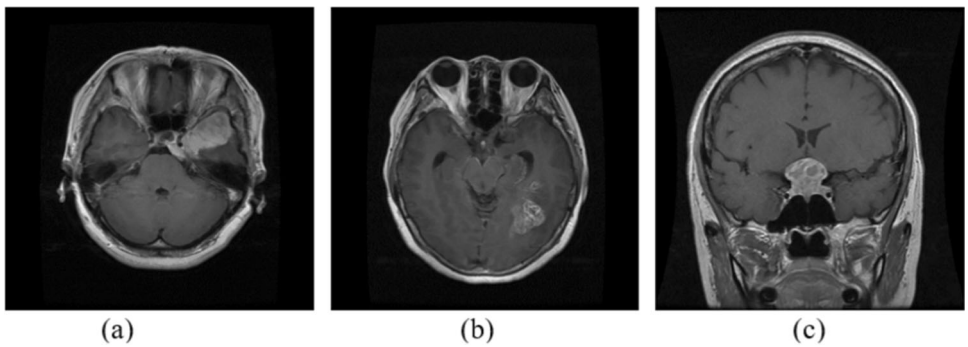

Fig. 2 MRI images of three different brain tumors: **a** meningioma; **b** glioma; and **c** pituitary

truth bounding box and returns a score. The higher the score is, the more accurately the model detects.

$$\text{mAP} = \frac{1}{n}\sum_{k=1}^{k=n}(\text{AP}_k) \tag{2}$$

The YOLOv3 model used in this study is based on the Darknet-53 model with sequential 3 × 3 and 1 × 1 53 convolution layers for feature extraction. This model gives faster and more accurate results when compared to Darknet-19-based YOLOv2 [47, 49].

3.3 Transfer learning

Deep learning, a subfield of machine learning, has the ability to analyze multi-dimensional features for prediction and detection tasks [50]. CNN produces remarkable results in image classification, object detection, and segmentation [51] problems and performs quite on images [2, 52]. In this study, the transfer learning approach was used in the training of pre-trained CNN models. The basic idea of this approach is to transfer information extracted from one domain to another target problem. Usually, a pre-trained network is chosen as the starting point for tackling a new problem. Rather than training a new network from scratch with randomly initialized weights, fitting a network with a transfer learning approach is quick and easy [53]. In this study, five popular and powerful state-of-the-art CNN architectures are used for the task of classifying and identifying brain tumors on the MRI images.

DenseNet201 [54], a pre-trained CNN model has 201 deep layers. While the traditional CNN has a total of L connections, one connection between each layer, DenseNet201 has $L(L + 1)/2$ direct connections. The feature maps extracted from all previous layers are used as input for each layer. This architecture has the significant advantages of mitigating the vanishing gradient problem, enhancing feature propagation, promoting feature reuse, and significantly reducing the number of parameters.

ResNet50 [55], which includes 50 deep layers, has been introduced to facilitate the training of deep networks.

Specific skip connections or shortcuts are used to jump over some layers. Residual functions that learn layer inputs by reference are used in the layers. ResNet50V2 [56] is a version of ResNet50 with changes in propagation formulation of connections between blocks and offers better performance than ResNet50.

The InceptionV3 architecture which is another pre-trained CNN has 48 convolution layers, symmetrical and asymmetrical building blocks, average/max pooling, and fully connected layers [57]. Batch normalization is applied throughout the architecture and Softmax is used as the loss function. Basically, InceptionV3 works more simply and efficiently by resolving sets of operations that take into account inter-layer and spatial correlations separately.

The VGG16 and VGG19 models [58] are convolutional neural network architectures that were developed at the Visual Geometry Group Network Oxford Robotics Institute.

The VGG16 architecture consists of 16 convolutional layers and three fully connected layers. It also has five max-pooling layers of 2 × 2 in each convolution layer [19]. VGG19 architecture consists of five building blocks. The first and second building blocks include 2 convolutional layers and 1 pooling layer. The third and fourth blocks have 4 convolutional layers and 1 pooling layer. The last block consists of 4 convolutional layers. In addition, 3 × 3 filters are used in this architecture [59].

3.3.1 Bi-LSTM

Traditional LSTM presents previous data as it only receives inputs in the backward direction through hidden states [60]. The Bi-LSTM network differs from one-way LSTM which only has backward propagation to obtain preliminary information on temporal data [61]. Bi-LSTM network trains LSTM networks in direction of forward and backward simultaneously and can extract past and future time features of the sample simultaneously to get better prediction results than LSTM [20]. In other words, the output layer of the LSTM network obtains the information from the input data at time t and the backward hidden state ($t-1$, $t-2$, … ,$t-N$), while the bidirectional LSTM network additionally uses the forward hidden state ($t + 1$, $t + 2$).,… ,$t + N$) [62]. The general structure of Bi-LSTM is shown in Fig. 3.

A multi-input and multi-output strategy can be created with the batch-input and batch-output features of each LSTM network. Bi-LSTM trains an n-step prediction model F from the time series as can be seen in Eq. 3 [63]:

$$[\widehat{x}_{t+1}, \widehat{x}_{t+2}, \ldots, \widehat{x}_{t+n}] = F(x_1, x_2, \ldots i, x_t) \tag{3}$$

Here, × 1, × 2,…,x_t are the n-step prediction results of the Bi-LSTM model under multi-input and multi-output strategy.

3.4 Performance metrics

Three types of brain tumors are examined in this study. In such multi-class problems, the average of the measurements obtained for each class is taken. When calculating these measurements, the class considered is regarded as positive, and other classes as negative. In this framework, metrics between Eqs. 4 and 7 are calculated for each class. Here, TN, TP, FN, and FP, which are employed for calculation of the measures such as accuracy and sensitivity,

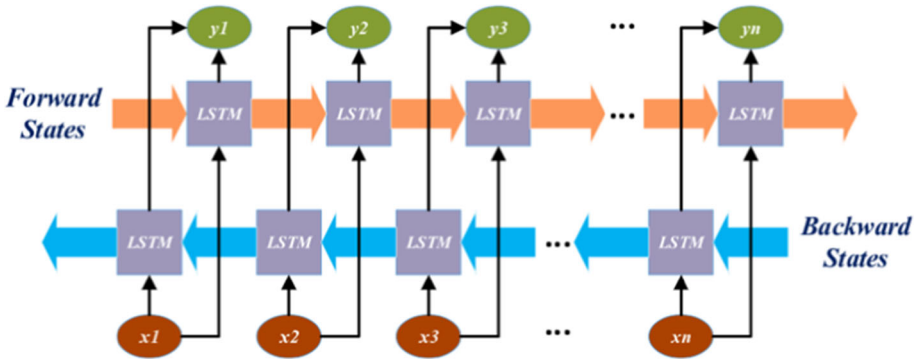

Fig. 3 Bi-LSTM network architecture [63]

etc., denote the number of true-negative, true positive, false negative, and false positive, respectively. Then, as given between Eqs. 8 and 11, the classification performances of the models are calculated by averaging the metrics obtained.

For a class k,

$$\text{Sen}(k) = \frac{\text{TP}(k)}{\text{TP}(k) + \text{FN}(k)} \tag{4}$$

$$\text{Spe}(k) = \frac{\text{TN}(k)}{\text{TN}(k) + \text{FP}(k)} \tag{5}$$

$$\text{Acc}(k) = \frac{\text{TP}(k) + \text{TN}(k)}{\text{TP}(k) + \text{FN}(k) + \text{TN}(k) + \text{FP}(k)} \tag{6}$$

$$\text{Pre}(k) = \frac{\text{TP}(k)}{\text{TP}(k) + \text{FP}(k)} \tag{7}$$

$$\text{Average Sen} = \frac{1}{\#\text{classes}} \sum_{k=1}^{\#\text{classes}} \text{Sen}(k) \tag{8}$$

$$\text{Average Spe} = \frac{1}{\#\text{classes}} \sum_{k=1}^{\#\text{classes}} \text{Spe}(k) \tag{9}$$

$$\text{Average Acc} = \frac{1}{\#\text{classes}} \sum_{k=1}^{\#\text{classes}} \text{Acc}(k) \tag{10}$$

$$\text{Average Pre} = \frac{1}{\#\text{classes}} \sum_{k=1}^{\#\text{classes}} \text{Pre}(k) \tag{11}$$

4 Experiments

4.1 Experimental setup

Training and testing processes of YOLO detection algorithm, pre-trained CNN and Bi-LSTM models in this study were carried out, using Tensorflow and Keras Library in Python on Google Colab with Tesla P100-PCIE-16 GB GPU, Intel(R) Xeon(R) 2.30 GHz CPU and 25 GB Ram system components. The training of the models YOLO, pre-trained CNN and Bi-LSTM and also parameters of them are presented in detail below.

4.2 Image pre-processing

Since the brain tumor MRI images used in the study were published as MATLAB '.mat' file, these files were first to read with the "pymatreader" library in the Python programming language. Then, the images were resized to $299 \times 299 \times 3$ for the InceptionV3 pre-trained CNN model, while $224 \times 224 \times 3$ is for other pre-trained models. In addition, one hot encoding is applied to the output class labels.

4.3 YOLO object detection

For training of the YOLO detection algorithm, the brain region in the image must be labeled. Labeling was made with the 'labelImg' (https://github.com/tzutalin/labelImg) graphical image annotation tool. In this process, the height (bH), width (bW) of the brain images and the position of

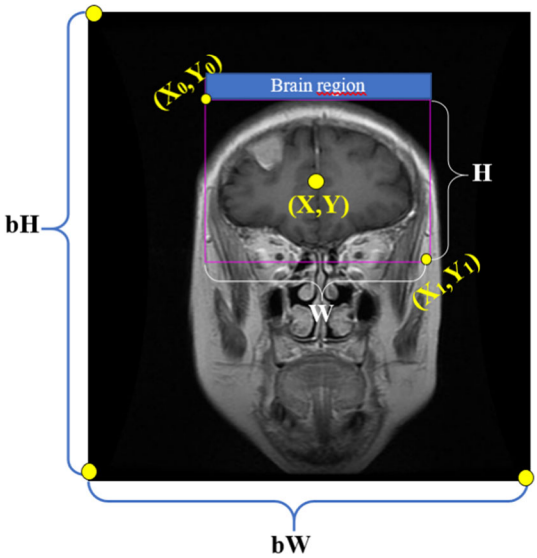

Fig. 4 Coordinate information calculated on the labeled brain image

the brain region (X_0, Y_0, X_1, Y_1) were saved in the text file. Afterward, the data were made ready for YOLO by applying the normalization process. For this, the center coordinates (X, Y), height (H) and width (W) of the labeled brain region shown in Fig. 4 are calculated as in Eqs. 12 and 13 [64].

$$X = \frac{X_1 + X_0}{2} \times \frac{1}{\mathrm{bW}}, \quad Y = \frac{Y_1 + Y_0}{2} \times \frac{1}{\mathrm{bH}} \tag{12}$$

$$W = (X_1 - X_0) \times \frac{1}{\mathrm{bW}}, \quad H = (Y_1 - Y_0) \times \frac{1}{\mathrm{bH}} \tag{13}$$

A total of 1200 images which consisted of 400 images selected randomly from each class were labeled. Following the labeling and normalization processes, 70% and 30% of the labeled data were used for training and testing, respectively. Because YOLO performs extremely well in this training and test set, the remaining 1864 images were not included in YOLO's training and testing process. Model performance is evaluated based on mAP and IoU metrics. Bounding boxes above of certain IoU threshold are taken into account when evaluating according to the mAP metric. When taking into the account threshold value of 0.50, the mAP value for the test data was calculated as 100% and the average IoU value as 90.74%. According to these performance values, it can be said that the brain region is detected with high accuracy. Automatic detection of the brain region was performed by feeding all MRI images to the trained YOLO model. Then, this detected region was cropped with OpenCV and a new dataset was composed. Figure 5 presents the images of the brain region detected and cropped from MRI images with YOLO.

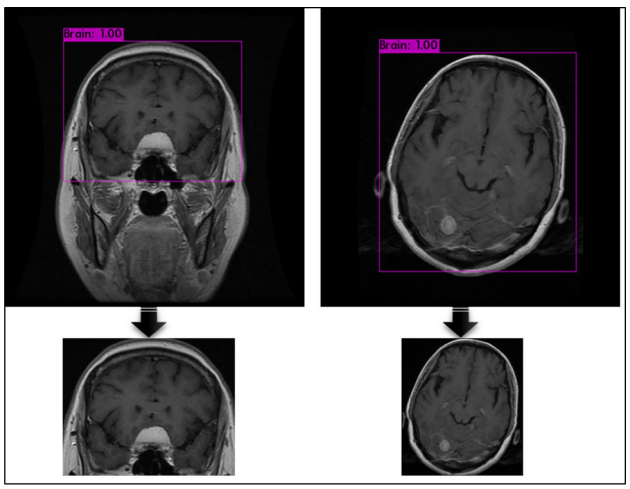

Fig. 5 Detection of brain regions from MRI images and cropping these regions

4.4 Deep features extraction

In order to train the Bi-LSTM based Model-2, deep features were extracted by feeding all MRI images cropped with the YOLO to the pre-trained CNN models. For this, the layers which are previous of the fully connected layer of DenseNet201, ResNet50V2, InceptionV3, VGG16, and VGG19 CNN models trained using the hold-out validation were used. The layers used to extract features and also the number of features obtained from these layers are shown in Fig. 6. 1920 features were obtained from the "global_average_pooling2d_12" layer of the DenseNet201 model, 2048 features from the "global_average_pooling2d" layers of the ResNet50V2 and InceptionV3 models, 25,088 features from the "flatten" layers of the VGG16 and VGG19 models.

4.5 Model training and testing

The training and testing process was carried out separately for the pre-trained CNN-based Model-1 fed with YOLO and Bi-LSTM-based Model-2 fed with the features obtained from Model-1. Tenfold cross-validation and hold-out techniques were used to identify the best model by more accurately revealing and comparing the performances of the models. In the hold-out technique, 60% of the dataset was used for training, 20% for validation, and the remaining part 20% for testing. Some parameters used in the training of pre-trained CNN and Bi-LSTM models are given in Table 1, and other parameters are used as default. Optimization is the learning algorithm that determines how millions or even billions of parameters should be updated [65]. In order to determine the best optimization algorithm, trial-and-error studies are usually performed during the training process [66]. In this context, Adam, Adadelta, Sgd, Rmsprop, Adamax, and Nadam optimizers were tested while building the models. While Adamax gives the highest classification performance on the DenseNet201 and ResnetV2 models, Sgd gives the highest classification performance on the others. The "Model Trainable" parameter is a parameter used in the convolution and pooling layers in pre-trained CNN models. If this parameter is "False," these layers are frozen and "imagenet" weights are used as they are. For this reason, this parameter is set to "True" in this study. Another important parameter in model training is the learning rate. When the learning rate is set too high, the prediction fluctuates. If this value is too small, the training time may be prolonged. As a result, different learning rates were tried, while the models were being trained, and the value that provided the best performance was determined. The Bi-LSTM network is trained at 100 epochs with parameters *rnn_width* = 64, *dropOut* =

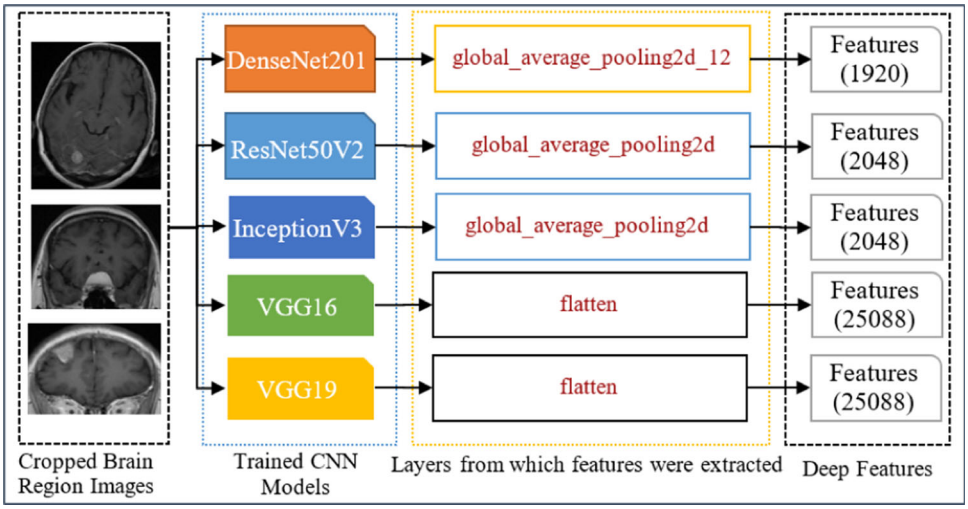

Fig. 6 Extraction of deep features

Table 1 Parameters setting of the Pre-trained CNN and Bi-LSTM models

Pre-trained CNN Model	Optimization Algorithm	Learning Rate	Batch Size	Epoch	Activation Function	Model Trainable	Loss Function
DenseNet201	Adamax	0.001	32	100	Relu	True	Categorical crossentropy
ResnetV2	Adamax	0.001	32	100	Softmax		
InceptionV3	Sgd	0.01	32	100			
VGG19	Sgd	0.01	32	100			
VGG16	Sgd	0.01	32	100			
Bi-LSTM	Sgd	0.01	32	100	Tanh		
	feature_count = 2048, class_count = 3, rnn_width = 64, dropOut = 0.1						

0.1, and also, the SGD optimizer algorithm was used with a learning rate of 0.01. Both hybrid models are trained and validated with the training and validation sets, respectively, and the classification performances of these models are compared with the test data. In order to make a general evaluation of the models, the overlapped confusion matrices were generated in the *k*-fold technique and the performance metrics of the models were calculated using these matrices. The overlapped CM is formed by summing CMs obtained in each fold.

Model-2 fed with the DenseNet201 features (YoDenBi-NET) for both hold-out and tenfold cross-validation gave the highest classification performance. By considering that presenting the curves of all folds will reduce the readability, the accuracy and loss curves of Fold-5 obtained by this model are available in Fig. 7. In both hold-out and tenfold cross-validation methods, it was observed that the accuracy value was close to one, and the loss value was close to zero between 30 and 40 epochs.

5 Results and discussion

In this study, brain tumor types were classified with YOLO and pre-trained CNN-based Model-1 and also YOLO, pre-trained CNN, and Bi-LSTM-based Model-2 approaches. The classification performances of these models are presented based on Recall, Precision, *F*1-score, and accuracy metrics in this section. For Model-1 and Model-2, Table 2 shows the tenfold cross-validation results and Table 3 shows the hold-out validation results.

According to the tenfold validation results, the YoDenBi-NET offered the highest classification performance with an average accuracy of 99.77%. This model correctly classified meningioma, glioma and pituitary brain tumors with the ratio of 99.44% ($R = 0.9944$), 99.86% ($R = 0.9986$), and 99.73% ($R = 0.9973$), respectively. As regards these ratios, it could be said that the model classifies all classes in a balanced and highly accurate manner. This is an indication that the model is well trained. In addition, in Model-1 fed with brain region images obtained from the YOLO detection algorithm, the DenseNet201 pre-trained CNN classified brain tumors with a 98.60% value

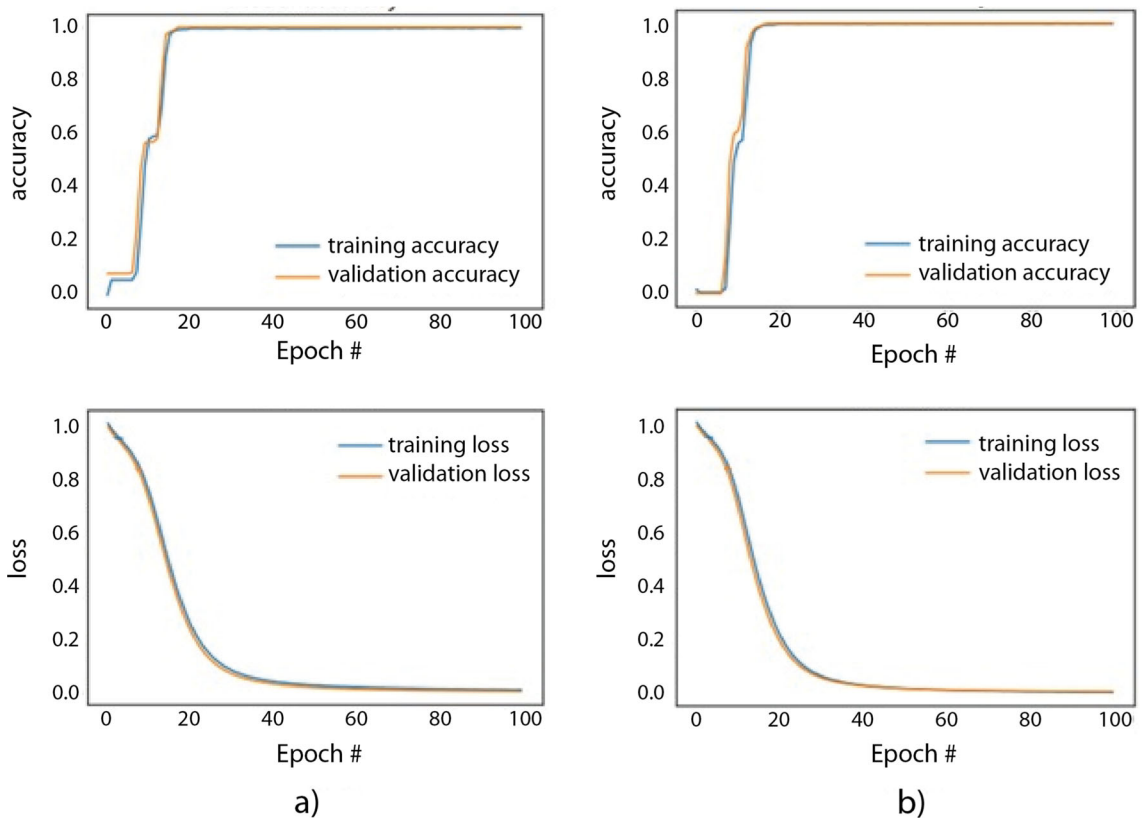

Fig. 7 Accuracy and loss curves of the YoDenBi-NET: **a** Hold-out technique results, **b** Fold-5 results

of accuracy. This rate is lower when compared to the YoDenBi-NET. That is, the Bi-LSTM-based Model-2, fed with the features obtained from Model-1, has improved its classification performance. The situation is similar when using ResNetV2, InceptionV3, VGG19, and VGG16 as the base model. In addition, the results obtained from the hold-out validation method support the results of the tenfold cross-validation. As a result, Model-1 and Model-2 including DenseNet201 pre-trained CNN have higher classification performance than others with 98.53% and 99.67%, respectively.

Confusion matrices of DenseNet201-based Model-1 and Model-2, where the highest classification performances were obtained, are presented in Figs. 8 and 9, respectively, for the tenfold and hold-out validation. Figure 8 presents the overlapped matrix. For tenfold cross-validation, Model-2 classified 704 of 708 meningioma tumors correctly and 4 incorrectly, while these values were 681 and 27 for Model-1, respectively. Model-2 has 1424 correct and 2 incorrect classifications for glioma tumor, while Model-1 has 1416 correct and 10 incorrect, respectively. Model-2 performed 929 correct and 1 incorrect classification for a pituitary tumor, while Model-1 performed 924 correct and 6 incorrect classifications. Findings supporting these results are valid for hold-out validation, as well. Accordingly, Model-2 misclassified only 1 of the meningioma tumor images, while Model-1 misclassified 7 of them. Model-2 correctly classified all glioma tumor images, while Model-1 misclassified 1 of them. Moreover, both Model 1 and Model 2 misclassified only 1 of the images containing the pituitary tumor. As a result, the experimental studies with both validation techniques show it is obvious that the Bi-LSTM-based Model-2, fed with the features obtained from YOLO-supported CNN models, significantly increases the classification performance.

It is important to reveal the effect of using the YOLO detection algorithm in the study on classification performance and training time. For this, DenseNet and DenseNet + BILSTM models, where the highest classification performance is obtained in this study, are also trained and tested on the raw dataset without YOLO. Both tenfold and hold-out validation methods were used during the training and testing of the models. According to the results, the CNN + Bi-LSTM model achieved 99.05% accuracy in tenfold cross-validation, while the basic CNN model achieved 98.29% accuracy. When compared to these models, the YOLO-supported CNN models improved by 0.72% and 0.31%, respectively, in tenfold cross-validation. Furthermore, the CNN + Bi-LSTM model provided 98.86% accuracy in the hold-out method, while the basic

Table 2 Tenfold cross-validation results of Model-1 and Model-2

Pre-trained model	Class	Performance results (%)							
		Model 2: YOLO + CNN + Bi-LSTM				Model-1: YOLO + CNN			
		R	*P*	*F*1	Average ACC	*R*	*P*	*F*1	Average ACC
DenseNet201	Overlapped								
	Meningioma	99.44	99.58	99.51	99.77	96.19	97.70	96.94	98.60
	Glioma	99.86	99.79	99.82		99.30	99.16	99.23	
	Pituitary	99.89	99.89	99.89		99.35	98.40	98.88	
	Average	99.73	99.75	99.74		98.28	98.42	98.35	
ResNetV2	Overlapped								
	Meningioma	97.60	98.57	98.08	99.08	96.05	96.18	96.11	98.07
	Glioma	99.30	99.16	99.23		98.67	98.88	98.77	
	Pituitary	99.89	99.36	99.62		98.71	98.29	98.50	
	Average	98.93	99.03	98.98		97.81	97.78	97.79	
InceptionV3	Overlapped								
	Meningioma	95.90	99.41	97.63	98.82	92.51	91.87	92.19	96.22
	Glioma	99.65	98.48	99.06		96.56	97.52	97.04	
	Pituitary	99.78	98.93	99.36		98.49	97.55	98.02	
	Average	98.45	98.94	98.68		95.86	95.65	95.75	
VGG19	Overlapped								
	Meningioma	97.60	97.60	97.60	98.66	94.63	95.58	95.10	97.36
	Glioma	98.95	99.09	99.02		97.90	98.80	98.34	
	Pituitary	99.03	98.82	98.93		98.60	96.53	97.55	
	Average	98.53	98.50	98.51		97.04	96.97	97.00	
VGG16	Overlapped								
	Meningioma	96.05	96.87	96.45	98.24	94.35	96.12	95.22	97.55
	Glioma	98.67	99.08	98.88		98.25	99.01	98.63	
	Pituitary	99.25	97.98	98.61		98.92	96.44	97.66	
	Average	97.99	97.98	97.98		97.17	97.19	97.17	

CNN model provided 96.08%. Yolo-supported models provided 0.81% and 2.45% improvement over these models, respectively. Furthermore, the CNN + Bi-LSTM model provided 98.86% accuracy in the hold-out method, while the base CNN model provided 96.08%. YOLO-supported models provided 0.81% and 2.45% improvement over these models, respectively. Cropping brain images with the YOLO model slightly increased the performance of the models. The main difficulty here is that the training of models on uncropped raw images takes an inordinate amount of time. It is quite high, especially for training the base CNN model. This time is 693 and 107 min for the tenfold cross-validation and hold-out methods, respectively. These times are 85 min and 11.4 min for YOLO-supported models, respectively. As a result, training time for YOLO-supported models is approximately 8–9 times shorter. This situation makes it impossible to test all of the hyperparameters in the models. Therefore, YOLO-supported models are stronger and fairer. These times are close in Bi-LSTM models fed with YOLO since the Bi-LSTM model is trained with the same features extracted from CNN. As a result, the training periods are approximately the same.

Brain tumor types could be classified by feature extraction from MRI images followed by a successful classification model. It is a known fact that features extracted from CNN's convolutional layers are more meaningful when compared to hand-craft features, in other words, strong distinctive features better represent the class of image. As can be seen in Table 4, deep learning-based studies are quite common in the literature. Some of these are studies in which hold-out [19–21, 34, 36, 37, 39, 41, 44, 67] and *k*-fold techniques [7, 23, 26, 38, 40, 41, 43, 44] are applied to the dataset used in our study.

Table 3 Hold-out test results of Model-1 and Model-2

Pre-trained model	Class	Performance results (%)							
		Model 2: YOLO + CNN + Bi-LSTM				Model-1: YOLO + CNN			
		R	*P*	*F*1	Average ACC	*R*	*P*	*F*1	Average ACC
DenseNet201	Meningioma	99.26	99.26	99.26	99.67	94.85	98.47	96.63	98.53
	Glioma	100	99.65	99.82		99.65	98.60	99.12	
	Pituitary	99.48	100	99.74		99.48	98.47	98.97	
	Average	99.58	99.64	99.61		97.99	98.51	98.24	
ResNetV2	Meningioma	98.57	99.28	98.92	99.35	94.85	95.56	95.20	97.88
	Glioma	99.32	100	99.66		98.94	98.25	98.59	
	Pituitary	100	98.33	99.16		98.45	98.96	98.71	
	Average	99.30	99.20	99.25		97.41	97.59	97.50	
InceptionV3	Meningioma	95	100	97.44	98.86	91.50	93.33	92.41	95.92
	Glioma	100	98.34	99.16		97.81	96.06	96.93	
	Pituitary	100	98.88	99.44		96.77	97.83	97.30	
	Average	98.33	99.07	98.68		95.36	95.74	95.55	
VGG19	Meningioma	95.62	97.76	96.68	98.37	93.67	94.27	93.97	96.41
	Glioma	99.01	99.34	99.17		96.42	98.18	97.29	
	Pituitary	99.42	97.18	98.29		98.86	95.60	97.21	
	Average	98.02	98.09	98.05		96.32	96.02	96.16	
VGG16	Meningioma	97.10	97.81	97.45	98.53	94.16	94.16	94.16	97.23
	Glioma	99.32	98.99	99.15		98.34	99	98.67	
	Pituitary	98.33	98.33	98.33		97.70	96.59	97.14	
	Average	98.25	98.38	98.31		96.73	96.58	96.66	

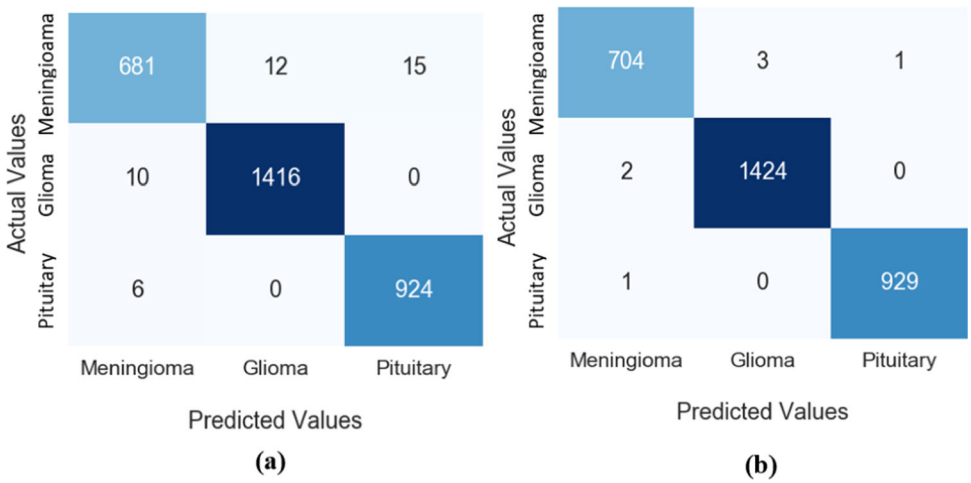

Fig. 8 Overlapped confusion matrices for tenfold cross-validation, **a** Model-1: YOLO-CNN (DenseNet201) model, **b** YoDenBi-NET

In hold-out experiments, the over-fitting or generalization problem of the model may occur, and therefore, the performance of the model may not be measured exactly. From studies with *K*-fold, Badža and Barjaktarović classified brain tumors with a CNN that was constructed from scratch [40]. Gumaei et al. trained the feedforward neural network classifier on the handcrafted features [23]. Paul et al. performed experiments that include fully connected neural networks, CNNs, and recurrent neural networks to classify brain tumor types. Moreover, the authors showed that state-of-the-art deep learning methods are more successful than traditional methods that need image pre-processing [38]. In another study, Pashaei et al. classified brain tumors with the kernel ELM classifier based on the features

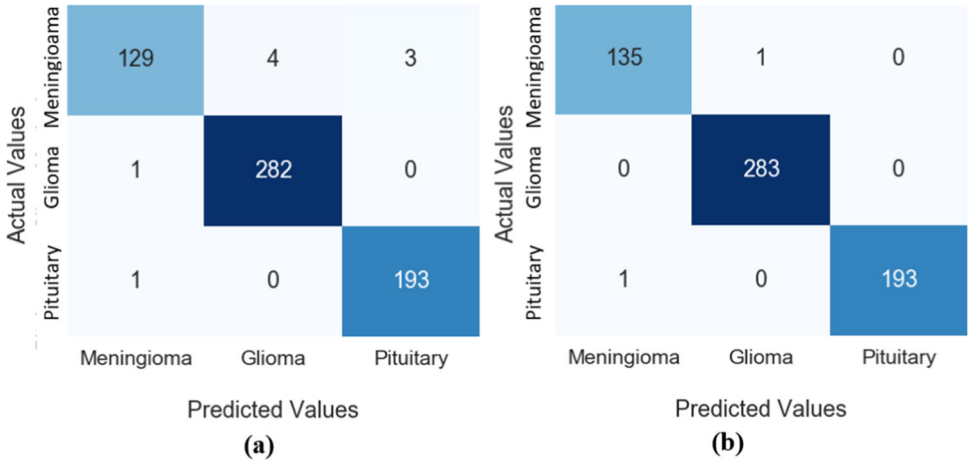

Fig. 9 Confusion matrices for hold-out validation, **a** Model-1: YOLO-CNN (DenseNet201) model, **b** YoDenBi-NET

Table 4 Comparison of the results of proposed model with related studies

Study	Method	*k*-fold cross-validation	Dataset	Acc (%)
Sachdeva et al. [24]	Principal Component Analysis and Artificial neural networks	Yes (k = 10)	Other	91
Yin et al. [25, 27]	Whale optimization algorithm and multilayer perceptual neural network-based classification	Yes (k = 5)	Other	87
Arı and Hanbay [27]	Extreme-learning machine-local receptive fields	No	Other	97.18
Ozyurt et al. [28]	Extreme Learning Machines	Yes (k = 10)	Other	98.33
Byale et al. [29]	Pre-processing and GLCM and Neural Network	No	Other	93.33
Anaraki et al. [32]	Convolutional Neural Networks and Genetic Algorithms	No	Other	94.2
Shanthi et al. [42]	Combined CNN-LSTM	No	Other	97.5
Vankdothu et al. [45]	CNN-LSTM	No	Other	92
Rehman et al. [19]	Fine-tuned VGG16	No	Same	98.69
Noreen et al. [20]	DensNet201	No	Same	99.51
Ismael and Abdel-Qader [34]	2D discrete wavelet transform and 2D Gabor filter and backpropagation neural network	No	Same	95.66
Kumar et al. [37]	Gray Wolf Optimization and Multiclass Support Vector Machines	No	Same	95.238
Das et al. [39]	CNN	No	Same	94.39
Huang et al. [21]	Random generated graph algorithms and CNN convolutional neural network	No	Same	95.49
Sultan et al. [36]	CNN	No	Same	98.7
Gumaei et al. [23]	Regularized extreme-learning machine	No	Same	94.233
		Yes (k = 5)		92.61
Pashaei et al. [26]	CNN and kernel ELM	Yes (k = 10)	Same	93.68
Paul et al. [38]	Deep learning	Yes (k = 5)	Same	91.43
Badža and Barjaktarović [40]	CNN	Yes (k = 10)	Same	96.56
Mondal and Shrivastava [41]	Parametric Flatten-p Mish activation function based deep CNN	No	Same	99.57 (Overall)
		Yes (k = 5)		98.45 (Overall)
Aamir et al. [43]	EfficientNet-B0,ResNet50	Yes (k = 5)	Same	98.95 (overall)
Aurna et al. [44]	Two stage ensemble CNN model	No	Same	99.20
		Yes(k = 8)		99.66
Öksüz et al. [7]	Expanded tumor region and pre-trained CNN	Yes (k = 5)	Same	97.25
Our method	**YoDenBi-NET**	**No**	**Same**	**99.67**
		Yes (k = 10)		**99.77**

Bold font indicates the results of our study

they obtained from the convolutional layers of CNN [26]. In addition, there are studies based on *k*-fold cross-validation on other datasets. For example, Sachdeva et al. trained the ELM classifier using the features they extracted with the SqueezeNet pre-trained CNN architecture [24]. Zou et al. applied feature reduction with the PCA technique on handcrafted features and then classified brain tumor types using artificial neural networks [68]. Özyurt et al. trained the multilayer perceptron neural network using the features they selected from the texture features, statistical features, and geometric features with the whale optimization algorithm [28]. With brain detection on the image by YOLO in the first stage, the deep features extraction by CNN for the detected regions in the second stage, and finally in the third stage, the classification process of the Bi-LSTM network which is another deep learning model, our study is unique and different from the studies in the literature.

6 Conclusion

In this study, YoDenBi-NET hybrid model was proposed to detect and classify brain tumor types from MRI images. The proposed model was trained with tenfold cross-validation and hold-out techniques on the MRI images containing three classes and evaluated using various performance measures such as accuracy, specificity, sensitivity, and *f*1-score. This model, which includes deep learning models at each stage, correctly classified 611 of 613 test images including meningioma, glioma, and pituitary tumors in the hold-out validation technique and has an overall classification accuracy of 99.67%. Moreover, according to the overlapped confusion matrix, the proposed model presented an average of 99.77% overall classification accuracy by correctly classifying 3057 out of 3064 images with the tenfold cross-validation technique. As a result, the Bi-LSTM network in the proposed model presented better overall classification accuracy, and this network significantly increased accuracy when compared to all YOLO-supported pre-trained models. The proposed model offered higher classification performance than studies in the literature that handled this problem on the same dataset. In future, it is aimed to build successful models with the ability to generalize on different and large datasets. In addition, segmentation of the brain tumor and then detection of the brain tumor type for the segmented region are among the targets.

Acknowledgements The authors would like to thank Cheng [46] to provide the public brain tumor dataset.

Funding None.

Availability of data and materials This study uses public dataset available at: https://figshare.com/articles/dataset/brain_tumor_dataset/1512427/5

Declarations

Conflict of interest The authors declare that they have no conflicts of interest.

References

1. Abdelaziz Ismael SA, Mohammed A, Hefny H (2020) An enhanced deep learning approach for brain cancer MRI images classification using residual networks. Artif Intell Med 102:101779. https://doi.org/10.1016/J.ARTMED.2019.101779
2. Kesav N, Jibukumar MG (2021) Efficient and low complex architecture for detection and classification of brain tumor using RCNN with two channel CNN. J King Saud Univ Comput Inf Sci 34(8):6229–6242. https://doi.org/10.1016/J.JKSUCI.2021.05.008
3. Biju KS, Hakkim HA, Jibukumar MG (2017) Ictal EEG classification based on amplitude and frequency contours of IMFs. Biocybern Biomed Eng 37:172–183. https://doi.org/10.1016/J.BBE.2016.12.005
4. Shafi ASM, Rahman MB, Anwar T et al (2021) Classification of brain tumors and auto-immune disease using ensemble learning. Inform Med Unlocked 24:100608. https://doi.org/10.1016/J.IMU.2021.100608
5. WHO (2022) Cancer. https://www.who.int/health-topics/cancer#tab=tab_1. Accessed 23 Feb 2022
6. Khairandish MO, Sharma M, Jain V et al (2021) A hybrid CNN-SVM threshold segmentation approach for tumor detection and classification of MRI brain images. IRBM 43(4):290–299. https://doi.org/10.1016/J.IRBM.2021.06.003
7. Öksüz C, Urhan O, Güllü MK (2022) Brain tumor classification using the fused features extracted from expanded tumor region. Biomed Signal Process Control 72(Part B):103356. https://doi.org/10.1016/J.BSPC.2021.103356
8. Sajjad M, Khan S, Muhammad K et al (2019) Multi-grade brain tumor classification using deep CNN with extensive data augmentation. J Comput Sci 30:174–182. https://doi.org/10.1016/J.JOCS.2018.12.003
9. Pereira S, Pinto A, Alves V, Silva CA (2016) Brain tumor segmentation using convolutional neural networks in MRI images. IEEE Trans Med Imaging 35:1240–1251. https://doi.org/10.1109/TMI.2016.2538465
10. Ahuja S, Panigrahi BK, Gandhi TK (2022) Enhanced performance of Dark-Nets for brain tumor classification and segmentation using colormap-based superpixel techniques. Mach Learn Appl 7:100212. https://doi.org/10.1016/J.MLWA.2021.100212
11. Pereira S, Meier R, Alves V, et al (2018) Automatic brain tumor grading from MRI data using convolutional neural networks and quality assessment. Lecture Notes in Computer Science (including subseries Lecture Notes in Artificial Intelligence and Lecture Notes in Bioinformatics). 11038 LNCS, pp 106–114. https://doi.org/10.1007/978-3-030-02628-8_12
12. Tandel GS, Tiwari A, Kakde OG (2021) Performance optimisation of deep learning models using majority voting algorithm for brain tumour classification. Comput Biol Med 135:104564. https://doi.org/10.1016/J.COMPBIOMED.2021.104564
13. Komaki K, Sano N, Tangoku A (2006) Problems in histological grading of malignancy and its clinical significance in patients with operable breast cancer. Breast Cancer 13(3):249–253. https://doi.org/10.2325/JBCS.13.249

14. Kaplan K, Kaya Y, Kuncan M, Ertunç HM (2020) Brain tumor classification using modified local binary patterns (LBP) feature extraction methods. Med Hypotheses 139:109696. https://doi.org/10.1016/J.MEHY.2020.109696
15. Tiwari A, Srivastava S, Pant M (2020) Brain tumor segmentation and classification from magnetic resonance images: review of selected methods from 2014 to 2019. Pattern Recognit Lett 131:244–260. https://doi.org/10.1016/J.PATREC.2019.11.020
16. Tandel GS, Biswas M, Kakde OG et al (2019) A review on a deep learning perspective in brain cancer classification. Cancers (Basel) 11(1):111. https://doi.org/10.3390/cancers11010111
17. Dora L, Agrawal S, Panda R, Abraham A (2018) Nested cross-validation based adaptive sparse representation algorithm and its application to pathological brain classification. Expert Syst Appl 114:313–321. https://doi.org/10.1016/J.ESWA.2018.07.039
18. Kumar S, Mankame DP (2020) Optimization driven deep convolution neural network for brain tumor classification. Biocybern Biomed Eng 40:1190–1204. https://doi.org/10.1016/J.BBE.2020.05.009
19. Rehman A, Naz S, Razzak MI et al (2020) A deep learning-based framework for automatic brain tumors classification using transfer learning. Circuits Syst Signal Process 39:757–775. https://doi.org/10.1007/S00034-019-01246-3/TABLES/8
20. Noreen N, Palaniappan S, Qayyum A et al (2020) A deep learning model based on concatenation approach for the diagnosis of brain tumor. IEEE Access 8:55135–55144. https://doi.org/10.1109/ACCESS.2020.2978629
21. Huang Z, Du X, Chen L et al (2020) Convolutional neural network based on complex networks for brain tumor image classification with a modified activation function. IEEE Access 8:89281–89290. https://doi.org/10.1109/ACCESS.2020.2993618
22. Cheng J, Huang W, Cao S et al (2015) Enhanced performance of brain tumor classification via tumor region augmentation and partition. PLoS One 10(12):e0140381. https://doi.org/10.1371/journal.pone.0140381
23. Gumaei A, Hassan MM, Hassan MR et al (2019) A hybrid feature extraction method with regularized extreme learning machine for brain tumor classification. IEEE Access 7:36266–36273. https://doi.org/10.1109/ACCESS.2019.2904145
24. Sachdeva J, Kumar V, Gupta I et al (2013) Segmentation, feature extraction, and multiclass brain tumor classification. J Digit Imaging 26:1141–1150. https://doi.org/10.1007/S10278-013-9600-0/TABLES/4
25. Yin B, Wang C, Abza F (2020) New brain tumor classification method based on an improved version of whale optimization algorithm. Biomed Signal Process Control 56:101728. https://doi.org/10.1016/J.BSPC.2019.101728
26. Pashaei A, Sajedi H, Jazayeri N (2018) Brain tumor classification via convolutional neural network and extreme learning machines. In: 2018 8th International conference on computer and knowledge engineering, ICCKE 2018. pp 314–319. https://doi.org/10.1109/ICCKE.2018.8566571
27. Arı A, Hanbay D (2018) Deep learning based brain tumor classification and detection system. Turk J Electr Eng Comput Sci 26:2275–2286. https://doi.org/10.3906/elk-1801-8
28. Özyurt F, Sert E, Avcı D (2020) An expert system for brain tumor detection: fuzzy C-means with super resolution and convolutional neural network with extreme learning machine. Med Hypotheses 134:109433. https://doi.org/10.1016/J.MEHY.2019.109433
29. Byale H, Lingaraju GM, Sivasubramanian S (2018) Automatic segmentation and classification of brain tumor using machine learning techniques. Int J Appl Eng Res (IJAER) 13:11686–11692
30. Hsieh KLC, Lo CM, Hsiao CJ (2017) Computer-aided grading of gliomas based on local and global MRI features. Comput Methods Programs Biomed 139:31–38. https://doi.org/10.1016/J.CMPB.2016.10.021
31. Zia R, Akhtar P, Aziz A (2018) A new rectangular window based image cropping method for generalization of brain neoplasm classification systems. Int J Imaging Syst Technol 28:153–162. https://doi.org/10.1002/IMA.22266
32. Anaraki AK, Ayati M, Kazemi F (2019) Magnetic resonance imaging-based brain tumor grades classification and grading via convolutional neural networks and genetic algorithms. Biocybern Biomed Eng 39:63–74. https://doi.org/10.1016/J.BBE.2018.10.004
33. Choudhury CL, Mahanty C, Kumar R, Mishra BK (2020) Brain tumor detection and classification using convolutional neural network and deep neural network. In: 2020 International conference on computer science, engineering and applications, ICCSEA 2020, pp 1–4. https://doi.org/10.1109/ICCSEA49143.2020.9132874
34. Ismael MR, Abdel-Qader I (2018) Brain tumor classification via statistical features and back-propagation neural network. In: IEEE International conference on electro ınformation technology 2018-May, pp 252–257. https://doi.org/10.1109/EIT.2018.8500308
35. Abiwinanda N, Hanif M, Hesaputra ST, et al (2019) Brain tumor classification using convolutional neural network. In: World congress on medical physics and biomedical engineering 2018. IFMBE proceedings, vol 68/1. Springer, Singapore, pp 183–189. https://doi.org/10.1007/978-981-10-9035-6_33
36. Sultan HH, Salem NM, Al-Atabany W (2019) Multi-classification of brain tumor images using deep neural network. IEEE Access 7:69215–69225. https://doi.org/10.1109/ACCESS.2019.2919122
37. Kumar A, Ansari MA, Ashok A (2019) A hybrid framework for brain tumor classification using grey wolf optimization and multi-class support vector machine. Int J Recent Technol Eng 8:7746–7752. https://doi.org/10.35940/ijrte.C6315.098319
38. Paul JS, Plassard AJ, Landman BA, Fabbri D (2017) Deep learning for brain tumor classification. vol 10137, pp 253–268. https://doi.org/10.1117/12.2254195
39. Das S, Aranya OFMRR, Labiba NN (2019) Brain tumor classification using convolutional neural network. In: 1st International conference on advances in science, engineering and robotics technology, vol 2019, pp 1–12. https://doi.org/10.1109/ICASERT.2019.8934603
40. Badža MM, Barjaktarović MČ (2020) Classification of brain tumors from MRI images using a convolutional neural network. Appl Sci 10(6):1999. https://doi.org/10.3390/app10061999
41. Mondal A, Shrivastava VK (2022) A novel Parametric Flatten-p Mish activation function based deep CNN model for brain tumor classification. Comput Biol Med 150:106183. https://doi.org/10.1016/J.COMPBIOMED.2022.106183
42. Shanthi S, Saradha S, Smitha JA et al (2022) An efficient automatic brain tumor classification using optimized hybrid deep neural network. Int J Intell Netw 3:188–196. https://doi.org/10.1016/J.IJIN.2022.11.003
43. Aamir M, Rahman Z, Dayo ZA et al (2022) A deep learning approach for brain tumor classification using MRI images. Comput Electr Eng 101:108105. https://doi.org/10.1016/J.COMPELECENG.2022.108105
44. Aurna NF, Yousuf MA, Taher KA et al (2022) A classification of MRI brain tumor based on two stage feature level ensemble of deep CNN models. Comput Biol Med 146:105539. https://doi.org/10.1016/J.COMPBIOMED.2022.105539
45. Vankdothu R, Hameed MA, Fatima H (2022) A brain tumor ıdentification and classification using deep learning based on CNN-LSTM method. Comput Electr Eng 101:107960. https://doi.org/10.1016/J.COMPELECENG.2022.107960

46. Cheng J (2017) Brain tumor dataset. figshare. Dataset. In: Figshare. https://figshare.com/articles/dataset/brain_tumor_dataset/1512427/5. Accessed 10 Nov 2021
47. Redmon J, Divvala S, Girshick R, Farhadi A (2016) You only look once: unified, real-time object detection. In: Proceedings of the IEEE computer society conference on computer vision and pattern recognition. Las Vegas, pp 779–788
48. Wu S, Yang J, Yu H, et al (2021) Gaussian guided IoU: a better metric for balanced learning on object detection. ArXiv 2103.13613
49. Redmon J, Farhadi A (2018) YOLOv3: an ıncremental ımprovement. arXiv:1804.02767v1. https://doi.org/10.48550/arXiv.1804.02767
50. Wainberg M, Merico D, Delong A, Frey BJ (2018) Deep learning in biomedicine. Nat Biotechnol 36(9):829–838. https://doi.org/10.1038/nbt.4233
51. Liu J, Li M, Lan W et al (2018) Classification of Alzheimer's disease using whole brain hierarchical network. IEEE/ACM Trans Comput Biol Bioinform 15:624–632. https://doi.org/10.1109/TCBB.2016.2635144
52. Ker J, Wang L, Rao J, Lim T (2017) Deep learning applications in medical image analysis. IEEE Access 6:9375–9379. https://doi.org/10.1109/ACCESS.2017.2788044
53. Manzo M, Pellino S (2021) Voting in transfer learning system for ground-based cloud classification. Mach Learn Knowl Extr 3(3):542–553. https://doi.org/10.3390/make3030028
54. Huang G, Liu Z, van der Maaten L, Weinberger KQ (2016) Densely connected convolutional networks. In: Proceedings - 30th IEEE conference on computer vision and pattern recognition, CVPR 2017 2017-Jan, pp 2261–2269. https://doi.org/10.48550/arxiv.1608.06993
55. He K, Zhang X, Ren S, Sun J (2016) Deep residual learning for ımage recognition. In: 2016 IEEE conference on computer vision and pattern recognition (CVPR). IEEE, pp 770–778
56. He K, Zhang X, Ren S, Sun J (2016) Identity mappings in deep residual networks. In: Lecture notes in computer science. pp 630–645
57. Szegedy C, Wei Liu, Yangqing Jia, et al (2015) Going deeper with convolutions. In: 2015 IEEE conference on computer vision and pattern recognition (CVPR). IEEE, pp 1–9
58. Simonyan K, Zisserman A (2014) Very deep convolutional networks for large-scale ımage recognition. arXiv:1409.1556. https://doi.org/10.48550/arXiv.1409.1556
59. Arshad H, Khan MA, Sharif MI, et al (2020) A multilevel paradigm for deep convolutional neural network features selection with an application to human gait recognition. Expert Syst 39(7): e12541. 1–21. https://doi.org/10.1111/exsy.12541
60. Joshi VM, Ghongade RB, Joshi AM, Kulkarni RV (2022) Deep BiLSTM neural network model for emotion detection using cross-dataset approach. Biomed Signal Process Control 73:103407. https://doi.org/10.1016/J.BSPC.2021.103407
61. Graves A (2013) Generating sequences with recurrent neural networks. arXiv:1308.0850. https://doi.org/10.48550/arxiv.1308.0850
62. Uçar E, Atila Ü, Uçar M, Akyol K (2021) Automated detection of Covid-19 disease using deep fused features from chest radiography images. Biomed Signal Process Control 69:102862. https://doi.org/10.1016/J.BSPC.2021.102862
63. Wei Y, Chen Z, Zhao C et al (2021) A BiLSTM hybrid model for ship roll multi-step forecasting based on decomposition and hyperparameter optimization. Ocean Eng 242:110138. https://doi.org/10.1016/J.OCEANENG.2021.110138
64. Aktaş A, Doğan B, Demir Ö (2020) Tactile paving surface detection with deep learning methods. J Fac Eng Archit Gazi Univ 35:1685–1700. https://doi.org/10.17341/gazimmfd.652101
65. An W, Wang H, Sun Q, et al (2018) A PID controller approach for stochastic optimization of deep networks. In: Proceedings of the IEEE computer society conference on computer vision and pattern recognition, pp 8522–8531. https://doi.org/10.1109/CVPR.2018.00889
66. Maas AL, Qi P, Xie Z et al (2017) Building DNN acoustic models for large vocabulary speech recognition. Comput Speech Lang 41:195–213. https://doi.org/10.1016/j.csl.2016.06.007
67. Ding S, Xu X, Nie R (2014) Extreme learning machine and its applications. Neural Comput Appl 25:549–556. https://doi.org/10.1007/S00521-013-1522-8/TABLES/1
68. Zou Q, Qu K, Luo Y et al (2018) Predicting diabetes mellitus with machine learning techniques. Front Genet 9:515. https://doi.org/10.3389/fgene.2018.00515